ACS APPLIED MATERIALS & INTERFACES

Research Article

www.acsami.org

Layer-by-Layer Assembly of Stable Aqueous Quantum Dots for Luminescent Planar Plate

Xuejing Zhang,[†] Changhua Zhou,*[,†] Shuaipu Zang,[†,‡] Huaibin Shen,[†] Pengpeng Dai,[‡] Xintong Zhang,*[,‡] and Lin Song Li*[,†]

[†]Key Laboratory for Special Functional Materials of the Ministry of Education, Henan University, Kaifeng, 475004, P. R. China

[‡]Center for Advanced Optoelectronic Functional Materials Research, and Key Laboratory for UV-Emitting Materials and Technology of Ministry of Education, Northeast Normal University, Changchun 130024, P. R. China

Supporting Information

ABSTRACT: This work reports the fabrication of a luminescent planar plate based on stable aqueous quantum dots (QDs) and poly(diallyldimethylammonium chloride) (PDDA) via a layer-by-layer (LBL) assembly technique. Preparation of aqueous QDs with facile monoalkyl maleate amphiphilic surfactants as the coating agent is conducted by a robust and efficient phase-transfer method. The as-prepared aqueous QDs exhibit bright emission, and their surface has very large negative zeta potential values, which are useful for electrostatic LBL assembly. Red, green, and blue luminescent planar plates are successfully fabricated via LBL assembly of the monocolor QDs, respectively. Through accurately adjusting the relative proportion of each monocolor luminescent component, we obtain an inspiring luminescent planar plate, which emits bright white light with a color coordinate of (0.3509, 0.3483), a correlated color temperature (CCT) of 4766 K, and a high color rendering index (CRI, Ra) of 89.5 under the irradiation of UV light. Therefore, this paper reports a facile process for the design and preparation of luminescent planar plates, which have potential applications in display and solid-state lighting devices.

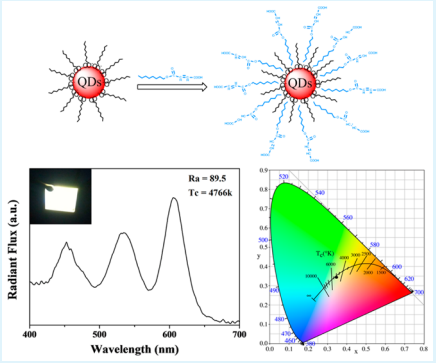

KEYWORDS: *monoalkyl maleate, water-soluble QDs, PDDA, LBL assembly, luminescent planar plates*

INTRODUCTION

Colloidal semiconductor quantum dots (QDs), as well as known as nanocrystals, have attracted great attention from engineers and scientists for their potential applications in the biomedical and optoelectronic fields.[1−5] Owing to the advantageous nature of QDs, including broad absorption, controllable photoemission, and superb photochemical stability, luminescent films based on QDs have been applied in a range of optic (or optoelectronic) devices, such as photodetectors,[6] photovoltaic devices,[7] light-emitting devices (LEDs),[8−11] and displays.[12] The properties of QDs film (thickness, structure, and accumulation mode) have a great influence on the performance of optic (or optoelectronic) devices. Therefore, how to evenly disperse QDs into films is the key technology.[13] So far, several methods have been explored to construct films, including spin-coating, vacuum thermal deposition, and drop-casting. Compared to these typical methods, the layer-by-layer (LBL) assembly is a popular and versatile protocol to prepare highly homogeneous films with tailored thickness, morphology, composites, and functionality.[14−16] The LBL assembly can control nanoscale composition and architectures through sequentially adsorbing of oppositely charged components.[17,18] The incorporation of QDs into a composite film via LBL assembly has been widely explored in order to obtain versatile luminescent materials. For instance, the fabrications of luminescent films based on QDs and polyelectrolyte have been proved to be a good method for various applications.[13,19−21] The hybrid luminescent films built by QDs and layered double hydroxides also have been reported.[22−24]

Usually, the LBL assembly is operated in aqueous solution, in which anionic and cationic materials are alternatively deposited on the substrate.[13,21] High-quality QDs are initially prepared as colloids in nonpolar organic solvents stabilized by hydrophobic ligands that result in the insolubility of them in aqueous solution. As a result, LBL assembly usually involves the phase transfer of hydrophobic QDs from nonpolar organic media to aqueous solution through ligand exchange.[25,26] However, aqueous QDs always lose their native stability and brightness after ligand exchange.[27−29] Compared to ligand exchange, the encapsulation of hydrophobic QDs can largely reduce the quantum yields (QYs) and colloidal stability loss of QDs. Although the encapsulations of hydrophobic QDs have been extensively researched, coating the hydrophobic QDs that are suitable for LBL assembly are still crucial issues to be resolved.[30−32]

Received: April 7, 2015
Accepted: June 19, 2015
Published: June 19, 2015

DOI: 10.1021/acsami.5b02957
ACS Appl. Mater. Interfaces 2015, 7, 14770−14777

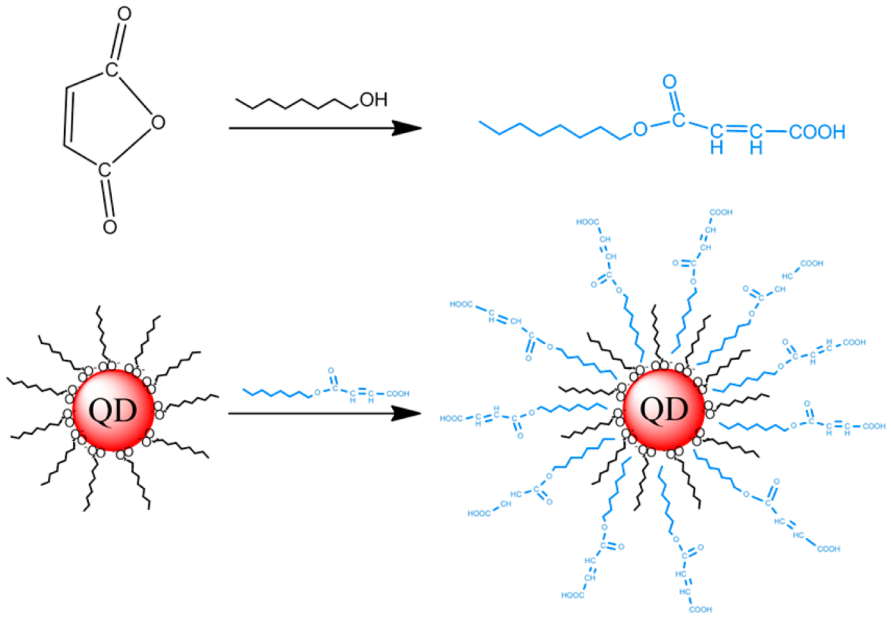

Figure 1. Synthesis of monoalkyl maleate surfactants through reaction between maleic anhydride and fatty alcohol (upper). Formation of water-soluble QDs using monoalkyl maleate surfactants (bottom).

In this work, we synthesize monoalkyl maleate amphiphilic surfactants with a simple one-step method. Monoalkyl maleate amphiphilic surfactants are first used as the coating agent to transfer hydrophobic QDs from nonpolar media into aqueous media. The obtained aqueous QDs with micellar structures have many carboxyl groups on their surfaces, resulting in large negative zeta potential values, which drive an electrostatic LBL assembly of these aqueous QDs and positively charged poly(diallyldimethylammonium chloride) (PDDA). Using the LBL self-assembly technique, we successfully prepare red, green, and blue luminescent planar plates with different layers of monocolor PDDA/QDs film on the glass slide. Moreover, through controlling the relative ratio of monocolor PDDA/QDs films, luminescent planar plates with white light emission are also prepared. The obtained luminescent planar plates can be potentially applied in the field of display and solid-state lighting.

EXPERIMENTAL SECTION

Materials. Cadmium oxide (CdO, 99.99%, powder), selenium (Se, 99.99%, powder), zinc oxide (ZnO, 99.9%, powder), sulfur (S, 99.98%, powder), 1-octadecene (ODE, 90%), poly(diallyldimethylammonium chloride) (PDDA), oleic acid (OA, 90%), and 1-octanethiol (OT, 98%) were purchased from Aldrich. Maleic anhydride (MA, AR), paraffin oil (AR), *n*-butyl alcohol (AR), sodium hydroxide (AR), *n*-octanol (AR), ammonia−water (28%), dodecanol (AR), hexane (AR), *n*-hexadecanol (AR), methanol (AR), heptane (AR), chloroform (AR), and concentrated sulfuric acid (98%) were purchased from Beijing Chemical Reagent Ltd., China.

Synthesis of Hydrophobic QDs. Original hydrophobic CdSe/ZnS QDs with red and green emission were prepared according to a "green" synthetic protocol (details in the Supporting Information).[33] Blue-emitting $Zn_xCd_{1-x}Se/ZnS$ QDs were synthesized according to ref 34 (details in the Supporting Information). The as-synthesized CdSe/ZnS and $Zn_xCd_{1-x}Se/ZnS$ QDs were purified using methanol and dispersed in $CHCl_3$ before further treatment.

Synthesis of Monoalkyl Maleate Surfactants. Monoalkyl maleate surfactants were synthesized with maleic anhydride and fatty alcohols.[35] In the synthesis of monooctyl maleate, maleic anhydride (49.03 g, 0.50 mol) and 1-octanol (65.12 g, 0.50 mol) were mixed and heated at 80 °C for 1 h. Heptane (120 mL) was poured into the reaction system and stirred for 15 min at 80 °C. Subsequently, the mixture was stirred at room temperature for 3 h and at 15 °C for 2 h. The trapped precipitate was recrystallized in the same way. The yield of monooctyl maleate was 63.58%. Monobutyl maleate, monododecyl maleate, and monohexadecyl maleate were also prepared in a similar way.

Surface Modification of Hydrophobic QDs. Using monoalkyl maleate surfactants as the coating agents, a simple procedure was provided for preparation of aqueous QDs. First, 0.01 g (7.0×10^{-4} mmol) of hydrophobic QDs was dispersed in chloroform (5 mL). Then, 0.16 g (7.0×10^{-1} mmol) of monooctyl maleate was added to the solution, and the mixture was stirred for 1 h in a closed flask under room temperature. Then, the chloroform was slowly removed by rotary evaporation, and the remaining surfactants-QDs were dispersed in NaOH solution (0.028 g of NaOH in 10 mL of deionized water) with 5 min sonication. Finally, a clear solution of aqueous QDs was obtained. This transfer process had a nearly 100% efficiency.

LBL Assembly of PDDA/QDs Films. The glass substrate (2.5 cm × 2.5 cm) was cleaned with water and then was dipped into concentrated sulfuric acid and concentrated NH_3/30% H_2O_2 (7:3) for 40 min each. LBL films were fabricated on the basis of the following cyclic process: the worked glass substrate was treated with the solution of PDDA (2.0 mg/mL) for 5 min and then was dipped into QDs solution (1.0 mg/mL, pH = 8) for another 5 min. In order to get the desired film with a controllable thickness, the cycle was repeated with the required number of times. Before the next step of the immersion process, it is necessary to rinse off the residual solution with deionized (DI) water. The resulting luminescent planar plates were dried with nitrogen at 25 °C.

Characterization. Photoluminescence (PL) spectra were collected using an Ocean Optics spectrophotometer (mode PC2000-ISA) under the excitation of 365 nm. The measurements of Fourier transform infrared (FTIR) spectra were done from films of a dried solution on KBr crystals with a Nicolet AVATAR 360 spectrometer. The morphology and size of QDs were measured with a JEM 100CX-II transmission electron microscope (TEM) at 100 kV. Zeta potential data were recorded using a Zetasizer Nano-ZS (Malvern Instruments, U.K.) at 25 °C. Thermogravimetric analysis (TGA) of the QDs were taken on a Mettler Toledo TGA/SDTA 851e under the temperature range of 20−600 °C at a heating rate of 10 °C/min in a N_2 atmosphere. The PL QYs of hydrophobic QDs and aqueous QDs were measured using Rhodamin 6G that have known emission

DOI: 10.1021/acsami.5b02957
ACS Appl. Mater. Interfaces 2015, 7, 14770−14777

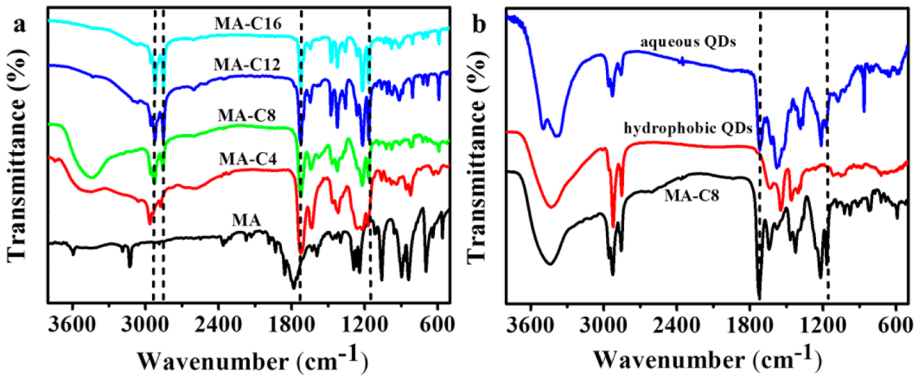

Figure 2. (a) FTIR characterizations of monoalkyl maleate: maleic anhydride (MA), monobutyl maleate (MA-C4), monooctyl maleate (MA-C8), monododecyl maleate (MA-C12), and monohexadecyl maleate (MA-C16). (b) FTIR characterizations of monooctyl maleate (MA-C8), hydrophobic QDs, and corresponding monooctyl maleate modified QDs.

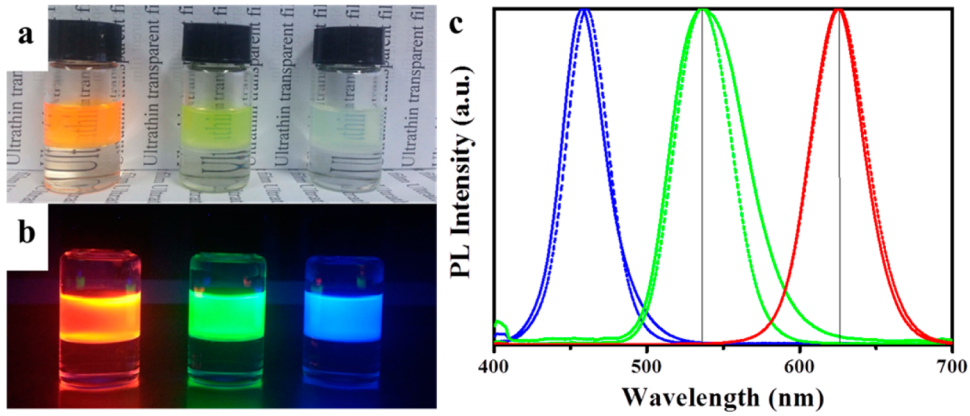

Figure 3. Photographs of red (CdSe/ZnS-625 nm), green (CdSe/ZnS-535 nm), and blue ($Zn_xCd_{1-x}Se$/ZnS-458 nm) MA-C8-QDs (upper phase is H_2O; bottom phase is $CHCl_3$) at room light (a) and 365 nm ultraviolet light (b). Comparison of the PL sprectra of red, green, and blue initial hydrophobic QDs (dashed line) and corresponding MA-C8-QDs (solid line) (c).

efficiencies as reference standard. PL characteristics of the white-emitting planar plate, such as PL spectrum, CCT, Commission Internationale de l'Eclairage (CIE) color coordinates, and CRI, were measured using a fiber optic spectrometer (Ocean Optics USB 4000) with an integrated sphere at room temperature.

RESULTS AND DISCUSSION

Preparation of Monoalkyl Maleate Surfactants and Hydrophilic QDs. The procedure for synthesizing monoalkyl maleate surfactants is illustrated in Figure 1 (upper). By this method, we prepared monobutyl maleate, monoocty maleate, monododecyl maleate, and monohexadecyl maleate, respectively. This synthetic process was facile, efficient, and available for large-scale production. FTIR spectroscopy was applied to validate the formation of monoalkyl maleates, as shown in Figure 2a. The appearance of the 1725 cm^{-1} peak and the disappearance of the 1775 cm^{-1} peak were attributed to the new formation of −COOH and the complete decomposition of anhydride. A band at 1172 cm^{-1} for monoalkyl maleate that can be assigned to the C−O−C vibration mode was observed, indicating that an ester group was formed after the reaction of maleic anhydride and fatty alcohol. For monoalkyl maleate samples, the appearance of the 2940 and 2850 cm^{-1} peak was attributed to the alkyl chain of monoalkyl maleate. The ^1H NMR spectra of monoalkyl maleate samples are presented in Figure S1 of the Supporting Information.

The process for preparing aqueous QDs is showed in Figure 1 (bottom). We mixed the monoalkyl maleate surfactants and QDs in chloroform, evaporated the solvent, and followed with the addition of aqueous buffer. Monoalkyl maleate contains both a hydrophobic chain ($-OC_nH_{2n+1}$) and a carboxylic acid group. The hydrophobic chain ($-OC_nH_{2n+1}$) was used to connect with the hydrophobic ligand of QDs through van der Waals interactions, and the carboxylic acid group was available for the dissolution of modified QDs in aqueous solution. The van der Waals interaction is very important for the stability of QDs in water. In principle, the van der Waals interactions between hydrophobic ligands of QDs and the alkyl chains of monoalkyl maleate surfactants become greater with the increase of alkyl chain length. Consequently, the molar ratio of monoalkyl maleate surfactants to QDs and the length of alkyl chain should be considered in the preparation. When monobutyl maleate (4 carbons) surfactant was used as the coating agent, phase transfer was unsuccessful regardless of changing the molar ratio of surfactant to QDs from 300:1 to 2000:1. For monooctyl maleate (8 carbons) surfactant, a 1000:1 molar ratio of surfactant to QDs induces a nearly 100% transfer yield and forms a clear and stable solution of aqueous QDs. As for monododecyl maleate (12 carbons) and monohexadecyl maleate (16 carbons) surfactants, although a 1000:1 molar ratio of surfactants to QDs can achieve complete phase transfer, the obtained solution looks more like a hydrogel due to the high viscosity of monododecyl maleate and

DOI: 10.1021/acsami.5b02957
ACS Appl. Mater. Interfaces 2015, 7, 14770−14777

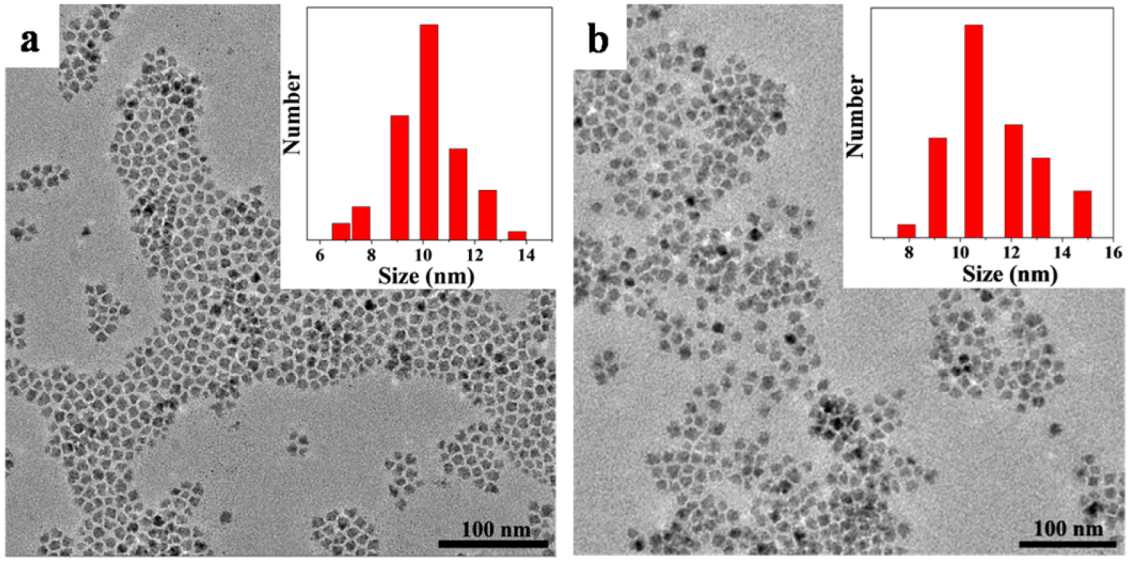

Figure 4. TEM images of the hydrophobic QDs in chloroform (a) and corresponding MA-C8-QDs in water (b). Inset: size distribution data.

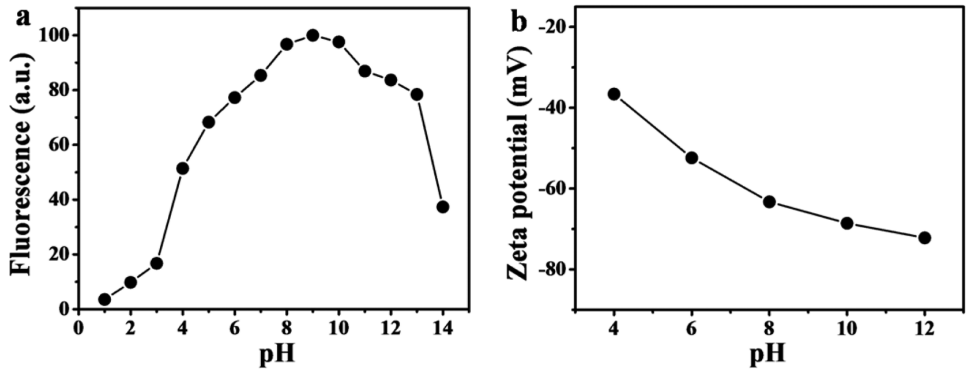

Figure 5. Changes of PL intensity of MA-C8-QDs in the range of pH (a) and pH-dependent zeta potential of MA-C8-QDs (b).

monohexadecyl maleate. Reducing the ratio of surfactants to QDs could not get satisfactory transfer efficiency. Therefore, the following discussion is always based on monooctyl maleate-QDs (MA-C8-QDs).

The functional groups presented on the surface of MA-C8-QDs and original QDs are also characterized with FTIR spectroscopy (Figure 2b). Compared to original QDs sample, MA-C8-QDs sample have several new peaks (e.g., 1172, 1725 cm^{-1}), which also appear in the isolated monooctyl maleate sample. This result indicates that the surface of QDs has been successfully coated with monooctyl maleate. The analysis (TGA) gives compelling evidence that the proportion of monooctyl maleate in hydrophilic QDs (MA-C8-QDs) is about 50% (shown in Figure S2 of the Supporting Information).

Figure 3a shows the red, green, and blue MA-C8-QDs aqueous solutions under room light. This picture validates that MA-C8-QDs aqueous solutions are stable and clear. It was the visual evidence that hydrophobic QDs were completely transferred from the organic phase to the aqueous phase. These MA-C8-QDs exhibited bright light under a UV (365 nm) lamp (Figure 3b). The changes of PL spectra were then monitored (Figure 3c). All MA-C8-QDs have slight peak shifts (<2 nm) compared with the corresponding hydrophobic QDs. Compared to the full width at half-maximum (fwhm, 43 nm) of green hydrophobic QDs, the PL spectrum of green MA-C8-QDs (peak at 535 nm) has an increased fwhm (56 nm). Spectral shift and broadening may be caused by MA-C8, which existed in the proximity of the QDs' surface. Meanwhile, PL intensity and PL QY were slightly reduced after phase transfer (4% and 6% for red QDs, 10% and 16% for green QDs, 16% and 18% for blue QDs). Popularly, the phase-transfer step can cause great reduction of QYs. The retention of high QYs (>80%) of hydrophobic QDs confirmed the advantages of our method to prepare highly stable water-soluble QDs. PL QY and full width at half-maximum (fwhm) before and after surface modification with MA-C8 are collected in Table S1 of the Supporting Information. The different performance of the three colors QDs may attribute to initial hydrophobic QDs with surface passivation in different degrees. The obtained MA-C8-QDs aqueous solutions were stable without aggregation and change of optical properties for at least one year when they were stored under daylight.

Figure 4 presents the transmission electron microscopy (TEM) images of hydrophobic QD and corresponding MA-C8-QDs. Hydrophobic QDs predominantly consisted of individual particles with an average diameter of 10 nm (Figure 4a). The monodisperse MA-C8-QDs were observed without an evident change of size and shape relative to the original hydrophobic QDs (Figure 4b). TEM images confirm the nonaggregated nature of MA-C8-QDs. The size distributions were calculated by statistics from their corresponding TEM images.

DOI: 10.1021/acsami.5b02957
ACS Appl. Mater. Interfaces 2015, 7, 14770−14777

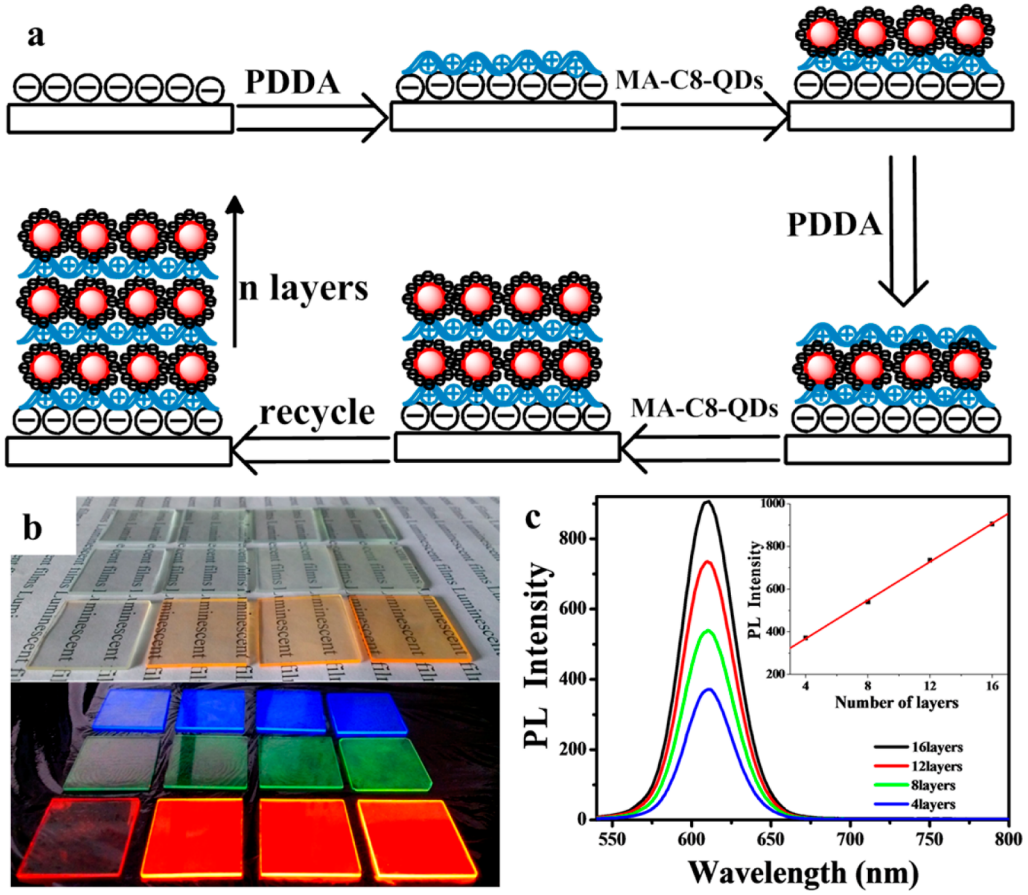

Figure 6. Schematic diagram of LBL assembly procedure (a). Photos of red, green, and blue PDDA/QDs luminescent planar plate under room light and 365 nm ultraviolet lamp (from left to right, the number of layers were 4, 8, 12, and 16, respectively.) (b). PL spectra of the red PDDA/QDs luminescent planar plates with different number of layers (c, inset: PL intensity of red PDDA/QDs luminescent planar plates versus the number of layers).

Stability of the Hydrophilic QDs. In order to assess the stability of MA-C8-QDs, the change of PL intensity was measured over the pH range of 1−14 (Figure 5a). As seen from Figure 5a, at low or high pH values (pH 1−5 or pH 14), the samples lost the stability. Highly acidic or alkali conditions result in a high ionic strength of the water environment, which is unfavorable to maintain stability of MA-C8-QDs with a micellar structure, and then the surface passivation layer of QDs may be destroyed by the existent overfull hydrogen ion or hydroxide ion. High acidity also gives rise to carboxyl protonation, drop of surface potential, and then instability of MA-C8-QDs in water. MA-C8-QDs are relatively stable over the pH range of 6−13, which may attribute to the essentiality of MA-C8-QDs, similar to the micellar structure where abundant carboxyl groups on the surface of MA-C8-QDs offer charge balance. At pH 8, MA-C8-QDs have the strongest stability. In other pH ranges, the slight decrease of PL intensity may be caused by the same reason mentioned above, but the impact is relatively weak.

A zeta potential measurement was adopted to monitor the charged characteristic of the MA-C8-QDs at different pH values. As shown in Figure 5b, the MA-C8-QDs are always negatively charged in pH values above 4. Zeta potential analysis reveals that abundant monooctyl maleates have been attached to the surface of QDs. At higher pH values, the surface charges increase due to the deprotonation of terminal carboxylic groups. The zeta potential is often used to evaluate the stability of colloids stabilized by electrostatic repulsion.[36] Because colloids with the zeta potential (above +30 mV, or below −30 mV) is extensively believed to be stable in water, the MA-C8-QDs with a zeta potential of −36.6 to −72.2 mV (pH 4−12) are assigned to the stable colloid. Furthermore, such a negatively charged characteristic is very beneficial to the electrostatic LBL assembly.

Preparation of Red, Green, Blue, and White Luminescent Planar Plates. Figure 6a illustrates the LBL assembly procedure of PDDA and QDs. Monocolor PDDA/QDs luminescent planar plates were fabricated by alternate deposition of negatively charged monocolor MA-C8-QDs with positively charged PDDA on the glass slide. As shown in Figure 6b, the red, green, and blue PDDA/QDs luminescent planar plates were transparent under room light and exhibit enhanced brightness with the increase of the layers under a 365 nm UV lamp. The PL spectra (Figure 6c) of the red luminescent planar plates showed no observable broadening and shift for different layers, indicating that the optical properties of MA-C8-QDs were not affected by the assembly procedure. A linear dependence of the PL intensity of the red PDDA/QDs luminescent planar plates on the number of layers demonstrated that the MA-C8-QDs were uniformly adsorbed during the LBL assembly (Figure 6c, inset). The above-mentioned performances were also observed for green and blue PDDA/QDs luminescent planar plates (shown in Figures S3 and S4 of the Supporting Information). The thickness of red

DOI: 10.1021/acsami.5b02957
ACS Appl. Mater. Interfaces 2015, 7, 14770−14777

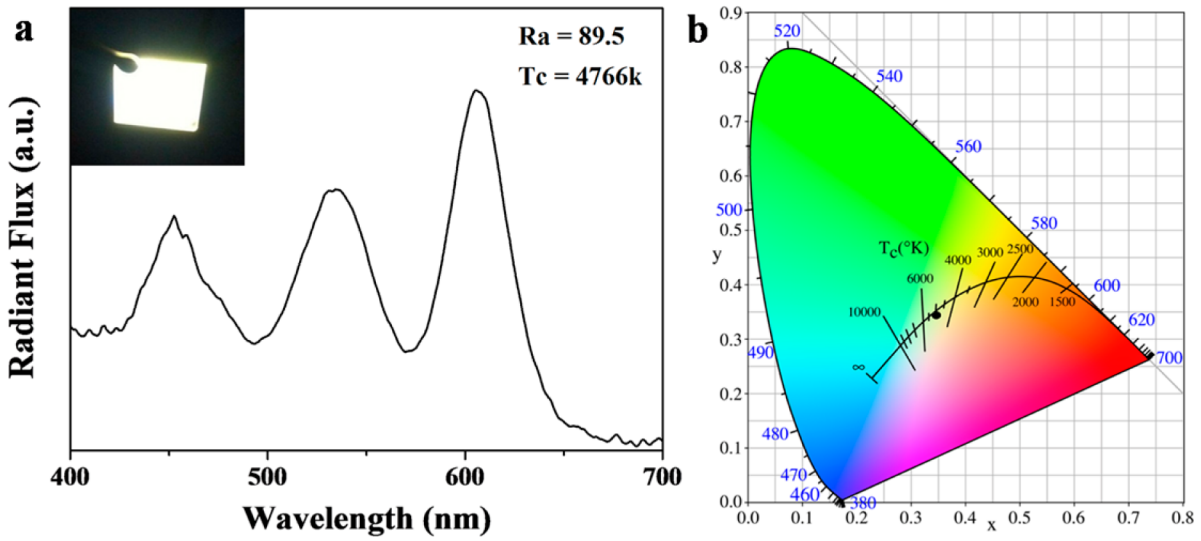

Figure 7. PL spectrum of white light planar plate with an excitation wavelength of 365 nm (a, inset: photo of the white light planar plate under 365 nm UV light). The CIE color coordinate of white light planar plate under the 365 nm excitation wavelength (b).

PDDA/QDs films was studied by SEM. The side-view SEM images showed that the thickness of red PDDA/QDs films increased with the increase of the number of layers (see Figure S5 in the Supporting Information). The almost linear rise confirmed the LBL assembly process. The estimated thickness of each red PDDA/QDs film is 32 nm.

Photostability and thermal stability are the key parameters for the applications of PL materials in various display and solid-state lighting devices. The photostability test was carried out by illuminating the red PDDA/QDs luminescent planar plates under an ultraviolet lamp, in comparison with the water solution of red MA-C8-QDs (see Figure S6 in the Supporting Information). After 2 h of irradiation, both solution and film maintained 90% of the initial PL intensity. For thermal stability tests, both solution and film can maintain 80% of the initial PL intensity after heating at 60 °C for 120 min (see Figure S7 in the Supporting Information). These results demonstrate that photostability and thermal stability of MA-C8-QDs almost have no change in the assembly process and the LBL assembled PDDA/QDs luminescent planar plates possess good ultraviolet and thermal resistance capability.

The acquisition of a luminescent planar plate with white light emission is crucial for applications in high-quality lighting and display devices. To minimize the influence of cascade excitation, we first assembled the red PDDA/QDs film and continued to assemble the green and blue PDDA/QDs film onto it. By accurately controlling the proportion of each monocolor film, we obtained the $[(\text{PDDA/QDs-610 nm})_6$-$(\text{PDDA/QDs-520 nm})_{12}(\text{PDDA/QDs-455 nm})_8]$ luminescent planar plate, which showed bright white light under a 365 nm ultraviolet lamp (Figure 7a, inset). The PL spectrum of the white light planar plate is shown in Figure 7a. This luminescent planar plate generated a high-quality white light with a high Ra of 89.5 and a relatively low CCT of 4766 K. The color coordinate was located at (0.3509, 0.3483), as shown in Figure 7b. The thickness of this white luminescent planar plate estimated with the side-view SEM is 1.02 μm. These results demonstrate that LBL assembly of MA-C8-QDs and PDDA can obtain luminescent material with controllable structure and color.

CONCLUSION

In summary, we have successfully prepared aqueous QDs by phase transfer of hydrophobic QDs from the organic phase to water using facile monoalkyl maleate amphiphilic surfactants as the encapsulating agent. Without exchanging initial surface ligands, the hydrophilic MA-C8-QDs preserved the PL properties of hydrophobic QDs. Furthermore, we have developed a simple and well-established approach for the preparation of polymer/QDs films. Red, green, and blue colors luminescent planar plates were fabricated by the LBL assembly of negatively charged stable MA-C8-QDs and positively charged PDDA on the glass slides, respectively. Especially, via precisely controlling the ratio between three monocolor films, we obtained a white luminescent planar plate with a high CRI value of 89.5, a relatively low CCT value of 4766 K, and the color coordinates at (0.3509, 0.3483). Overall, we have demonstrated a simple and highly efficient strategy for the fabrication of luminescent planar plates, which may find great application in the optical (or optoelectronic) field.

ASSOCIATED CONTENT

Supporting Information

The procedures for synthesizing red, green, and blue hydrophobic QDs and partial characterization data. The Supporting Information is available free of charge on the ACS Publications website at DOI: 10.1021/acsami.5b02957.

AUTHOR INFORMATION

Corresponding Authors

*E-mail: lsli@henu.edu.cn. Tel: +86-371-23881358. Fax: +86-371-23881358 (L.S.L.).
*E-mail: changhua@henu.edu.cn. Tel: +86-371-23881358. Fax: +86-371-23881358 (C.Z.).
*E-mail: xtzhang@nenu.edu.cn (X.Z.).

Notes

The authors declare no competing financial interest.

ACKNOWLEDGMENTS

The authors gratefully acknowledge the support of the National Natural Science Foundation of China (No. 21201055), Basic

DOI: 10.1021/acsami.5b02957
ACS Appl. Mater. Interfaces 2015, 7, 14770−14777

and cutting-edge technology research projects of Henan Province (No. 142300413207), the Program for Science & Technology Innovation Talents in Universities of Henan Province (No. 14HASTIT009), and the Program for Changjiang Scholars and Innovative Research Team in University (No. PCS IRT1126).

REFERENCES

(1) Supran, G. J.; Shirasaki, Y.; Song, K. W.; Caruge, J. M.; Kazlas, P. T.; Coe-Sullivan, S.; Andrew, T. L.; Bawendi, M. G.; Bulović, V. QLEDs for Displays and Solid-State Lighting. *MRS Bull.* **2013**, *38*, 703−711.

(2) Talapin, D. V.; Steckel, J. Quantum Dot Light-Emitting Devices. *MRS Bull.* **2013**, *38*, 685−691.

(3) Shirasaki, Y.; Supran, G. J.; Bawendi, M. G.; Bulović, V. Emergence of Colloidal Quantum-Dot Light-Emitting Technologies. *Nat. Photonics* **2013**, *7*, 13−23.

(4) Petryayeva, E.; Algar, W. R.; Medintz, I. L. Quantum Dots in Bioanalysis: A Review of Applications Across Various Platforms for Fluorescence Spectroscopy and Imaging. *Appl. Spectrosc.* **2013**, *67*, 215−252.

(5) He, X.; Ma, N. An Overview of Recent Advances in Quantum Dots for Biomedical Applications. *Colloids Surf., B* **2014**, *124*, 118−131.

(6) Osedach, T. P.; Zhao, N.; Geyer, S. M.; Chang, L. Y.; Wanger, D. D.; Arango, A. C.; Bawendi, M. C.; Bulović, V. Interfacial Recombination for Fast Operation of a Planar Organic/QD Infrared Photodetector. *Adv. Mater.* **2010**, *22*, 5250−5254.

(7) Jin, H.; Choi, S.; Lee, H. J.; Kim, S. Layer-by-Layer Assemblies of Semiconductor Quantum Dots for Nanostructured Photovoltaic Devices. *J. Phys. Chem. Lett.* **2013**, *4*, 2461−2470.

(8) Bae, W. K.; Kwak, J.; Lim, J.; Lee, D.; Nam, M. K.; Char, K.; Lee, C.; Lee, S. Multicolored Light-Emitting Diodes Based on All-Quantum-Dot Multilayer Films Using Layer-by-Layer Assembly Method. *Nano Lett.* **2010**, *10*, 2368−2373.

(9) Hong, S. P.; Park, H. Y.; Oh, J. H.; Yang, H.; Jang, S. Y.; Do, Y. R. Fabrication of Wafer-Scale Free-Standing Quantum Dot/Polymer Nanohybrid Films for White-Light Emitting Diodes Using an Electrospray Method. *J. Mater. Chem. C* **2014**, *2*, 10439−10445.

(10) Kwak, J.; Bae, W. K.; Lee, D.; Park, I.; Lim, J.; Park, M.; Cho, H.; Woo, H.; Yoon, D. Y.; Char, K.; Lee, S.; Lee, C. Bright and Efficient Full-Color Colloidal Quantum Dot Light-Emitting Diodes Using an Inverted Device Structure. *Nano Lett.* **2012**, *12*, 2362−2366.

(11) Kim, J. H.; Song, W. S.; Yang, H. Color-Converting Bilayered Composite Plate of Quantum-Dot−Polymer for High-Color Rendering White Light-Emitting Diode. *Opt. Lett.* **2013**, *38*, 2885−2888.

(12) Wood, V.; Panzer, M. J.; Chen, J.; Bradley, M. S.; Halpert, J. E.; Bawendi, M. G.; Bulović, V. Inkjet-Printed Quantum Dot−Polymer Composites for Full-Color AC-Driven Displays. *Adv. Mater.* **2009**, *21*, 2151−2155.

(13) Kim, D.; Okahara, S.; Shimura, K.; Nakayama, M. Layer-by-Layer Assembly of Colloidal CdS and ZnS-CdS Quantum Dots and Improvement of Their Photoluminescence Properties. *J. Phys. Chem. C* **2009**, *113*, 7015−7018.

(14) Suntivich, R.; Shchepelina, O.; Choi, I.; Tsukruk, V. V. Inkjet-Assisted Layer-by-Layer Printing of Encapsulated Arrays. *ACS Appl. Mater. Interfaces* **2012**, *4*, 3102−3110.

(15) Hammond, P. T. Form and Function in Multilayer Assembly: New Applications at the Nanoscale. *Adv. Mater.* **2004**, *16*, 1271−1293.

(16) DeRocher, J. P.; Mao, P.; Kim, J. Y.; Han, J.; Rubner, M. F.; Cohen, R. E. Layer-by-Layer Deposition of All-Nanoparticle Multilayers in Confined Geometries. *ACS Appl. Mater. Interfaces* **2012**, *4*, 391−396.

(17) Hammond, P. T. Engineering Materials Layer-by-Layer: Challenges and Opportunities in Multilayer Assembly. *AIChE J.* **2011**, *57*, 2928−2940.

(18) Franzl, T.; Klar, T. A.; Schietinger, S.; Rogach, A. L.; Feldmann, J. Exciton Recycling in Graded Gap Nanocrystal Structures. *Nano Lett.* **2004**, *4*, 1599−1603.

(19) Mamedov, A. A.; Belov, A.; Giersig, M.; Mamedova, N. N.; Kotov, N. A. Nanorainbows: Graded Semiconductor Films from Quantum Dots. *J. Am. Chem. Soc.* **2001**, *123*, 7738−7739.

(20) Wang, Y.; Tang, Z.; Correa-Duarte, M. A.; Liz-Marzán, L. M.; Kotov, N. A. Multicolor Luminescence Patterning by Photoactivation of Semiconductor Nanoparticle Films. *J. Am. Chem. Soc.* **2003**, *125*, 2830−2831.

(21) Lin, Y. W.; Tseng, W. L.; Chang, H. T. Using a Layer-by-Layer Assembly Technique to Fabricate Multicolored-Light-Emitting Films of CdSe@CdS and CdTe Quantum Dots. *Adv. Mater.* **2006**, *18*, 1381−1386.

(22) Liang, R.; Xu, S.; Yan, D.; Shi, W.; Tian, R.; Yan, H.; Wei, M.; Evans, D. G.; Duan, X. CdTe Quantum Dots/Layered Double Hydroxide Ultrathin Films with Multicolor Light Emission via Layer-by-Layer Assembly. *Adv. Funct. Mater.* **2012**, *22*, 4940−4948.

(23) Tian, R.; Liang, R.; Yan, D.; Shi, W.; Yu, X.; Wei, M.; Li, L. S.; Evans, D. G.; Duan, X. Intelligent Display Films with Tunable Color Emission Based on a Supermolecular Architecture. *J. Mater. Chem. C* **2013**, *1*, 5654−5660.

(24) Liang, R.; Yan, D.; Tian, R.; Yu, X.; Shi, W.; Li, C.; Wei, M.; Evans, D. G.; Duan, X. Quantum Dots-Based Flexible Films and Their Application as the Phosphor in White Light-Emitting Diodes. *Chem. Mater.* **2014**, *26*, 2595−2600.

(25) Jaffar, S.; Nam, K. T.; Khademhosseini, A.; Xing, J.; Langer, R. S.; Belcher, A. M. Layer-by-Layer Surface Modification and Patterned Electrostatic Deposition of Quantum Dots. *Nano Lett.* **2004**, *4*, 1421−1425.

(26) Jin, F.; Zheng, M. L.; Zhang, M. L.; Zhao, Z. S.; Duan, X. M. A Facile Layer-by-Layer Assembly Method for the Fabrication of Fluorescent Polymer/Quantum Dot Nanocomposite Thin Films. *RSC Adv.* **2014**, *4*, 33206−33214.

(27) Greytak, A. B.; Allen, P. M.; Liu, W.; Zhao, J.; Young, E. R.; Popović, Z.; Walker, B. J.; Nocera, D. G.; Bawendi, M. G. Alternating Layer Addition Approach to CdSe/CdS Core/Shell Quantum Dots with Near-Unity Quantum Yield and High On-Time Fractions. *Chem. Sci.* **2012**, *3*, 2028−2034.

(28) Liu, D.; Snee, P. T. Water-Soluble Semiconductor Nanocrystals Cap Exchanged with Metalated Ligands. *ACS Nano* **2011**, *5*, 546−550.

(29) Thiry, M.; Boldt, K.; Nikolic, M. S.; Schulz, F.; Ijeh, M.; Panicker, A.; Vossmeyer, T.; Weller, H. Fluorescence Properties of Hydrophilic Semiconductor Nanoparticles with Tridentate Polyethylene Oxide Ligands. *ACS Nano* **2011**, *5*, 4965−4973.

(30) Yang, J.; Dave, S. R.; Gao, X. Quantum Dot Nanobarcodes: Epitaxial Assembly of Nanoparticle-Polymer Complexes in Homogeneous Solution. *J. Am. Chem. Soc.* **2008**, *130*, 5286−5292.

(31) Qian, J.; Gao, X. Triblock Copolymer-Encapsulated Nanoparticles with Outstanding Colloidal Stability for siRNA Delivery. *ACS Appl. Mater. Interfaces* **2013**, *5*, 2845−2852.

(32) Zhou, C.; Yuan, H.; Shen, H.; Guo, Y.; Li, X.; Liu, D.; Xu, L.; Ma, L.; Li, L. S. Synthesis of Size-Tunable Photoluminescent Aqueous CdSe/ZnS Microspheres via a Phase Transfer Method with Amphiphilic Oligomer and Their Application for Detection of HCG Antigen. *J. Mater. Chem.* **2011**, *21*, 7393−7400.

(33) Shen, H.; Wang, H.; Tang, Z.; Niu, J. Z.; Lou, S.; Du, Z.; Li, L. S. High Quality Synthesis of Monodisperse Zinc-Blende CdSe and CdSe/ZnS Nanocrystals with a Phosphine-Free Method. *CrystEngComm* **2009**, *11*, 1733−1738.

(34) Shen, H.; Bai, X.; Wang, A.; Wang, H.; Qian, L.; Yang, Y.; Titov, A.; Hyvonen, J.; Zheng, Y.; Li, L. S. High-Efficient Deep-Blue Light-Emitting Diodes by Using High Quality $Zn_xCd_{1-x}S$/ZnS Core/Shell Quantum Dots. *Adv. Funct. Mater.* **2014**, *24*, 2367−2373.

(35) Hamaide, T.; Zicmanis, A.; Monnet, C.; Guyot, A. Synthesis and NMR Characterization of New Poly(ethoxyalkyl) Maleates. *Polym. Bull.* **1994**, *33*, 133−139.

(36) Kovalenko, M. V.; Bodnarchuk, M. I.; Zaumseil, J.; Lee, J. S.; Talapin, D. V. Expanding the Chemical Versatility of Colloidal

DOI: 10.1021/acsami.5b02957
ACS Appl. Mater. Interfaces 2015, 7, 14770−14777

Nanocrystals Capped with Molecular Metal Chalcogenide Ligands. *J. Am. Chem. Soc.* **2010**, *132*, 10085−10092.

DOI: 10.1021/acsami.5b02957
ACS Appl. Mater. Interfaces 2015, 7, 14770−14777